Int. J. Adv. Appl. Math. and Mech. 2(4) (2015) 25 - 34 (ISSN: 2347-2529)

Journal homepage: www.ijaamm.com

IJAAMM

International Journal of Advances in Applied Mathematics and Mechanics

Transient MHD free convection flow past a porous vertical plate in presence of viscous dissipation

Research Article

Siva Reddy Sheri *, **R.Srinivasa Raju**, **S. Anjan Kumar**

Department of Mathematics, GITAM University, Hyderabad Campus, Medak Dist., Telangana, India.

Received 14 November 2014; accepted (in revised version) 22 May 2015

Abstract: This article deals with the study of transient magnetohydrodynamic free convection flow past a vertical porous plate in presence of viscous dissipation. The governing differential equations are transformed into a set of non-linear coupled ordinary differential equations and solved using a Finite element method. The effects of various physical parameters on the dimensionless velocity, temperature and concentration profiles are depicted graphically and analyzed in detail. Also, the skin-friction, Nusselt number and Sherwood number at the plate of derived and discussed and their numerical values for various physical parameters are presented in tables. Favorable comparisons with previously published work on various special cases for different physical parameters.

MSC: 80A20 • 76R50 • 78A40

Keywords: Transient • MHD • Viscous dissipation • Finite element method

1. Introduction

The most common type of body force, which acts on a fluid, is due to gravity, so that the body force can be defined as in magnitude and direction by the acceleration due to gravity. Sometimes, electromagnetic effects are important. The electric and magnetic fields themselves must obey a set of physical laws, which are expressed by Maxwell's equations. The solution of such problems requires the simultaneous solution of the equations of fluid mechanics and electromagnetism. One special case of this type of coupling is known as magnetohydrodynamic.

Coupled heat and mass transfer phenomenon in porous media is gaining attention due to its interesting applications. The flow phenomenon in this case is relatively complex than that in pure thermal/solutal convection process. Processes involving heat and mass transfer in porous media are often encountered in the chemical industry, in reservoir engineering in connection with thermal recovery process, in the study of dynamics of hot and salty springs of a sea. Underground spreading of chemical waste and other pollutants, grain storage, evaporation cooling, and solidification are a few other application areas where combined thermosolutal convection in porous media are observed. However, the exhaustive volume of work devoted to this area is amply documented by the most recent books by Ingham and Pop[1], Nield and Bejan [2] and Vafai [3], Pop and Ingham [4] studied the problem of transient flow of a fluid past a moving semi-infinite vertical porous plate. However, many problem areas which are important in applications, as well as in theory still persist.

Convective heat transfer in porous media has been a subject of great interest for the last few decades. This interest was motivated by numerous thermal engineering applications in various disciplines, such as geophysical, thermal and insulation engineering, the modeling of packed sphere beds, the cooling of electronic systems, chemical catalytic records, ceramic processes, grain storage devices fiber and granular insulation, petroleum reservoirs, coal combustors, ground water pollution and filtration process. Kim [5] investigated an unsteady MHD convective heat transfer

* Corresponding author.
E-mail address: sheri7@gitam.edu (Siva Reddy Sheri)

Nomenclature

T'_w	Wall dimensional temperature
U'_∞	Dimensional free stream velocity
t'	Dimensional time
t	Time
u	Non âĂŞdimensional velocity
g	Acceleration due to gravity
K'	Dimensional porosity parameter
(u', v')	Dimensional velocity components
(x', y')	Dimensional Cartesian coordinates
C_p	Specific heat capacity
M	Magnetic parameter
Pr	Prandtl number
Gr	Thermal Grashof number
Gc	Solutal Grashof number
Sc	Schmidt number
E_c	Eckert number
D	Molecular diffusivity
C'_w	Wall dimensional concentration
C'_∞	Free stream dimensional concentration
U_0	Mean velocity
B_0	Magnetic field
S_0	Non dimensional Heat absorption parameter
S	Heat absorption parameter
u'_p	Plate velocity
n'	Dimensional free stream frequency of oscillation
U_∞	Free stream velocity
K	Permeability parameter
Nu	Nusselt numbe
Sh	Sherwood number

Greek symbols

β	Coefficient of Volume expansion
β^*	Volumetric coefficient of expansion with concentration
ν	Kinematic viscosity
σ	Electrical conductivity
ρ	Fluid density
k	Thermal conductivity
θ	Non âĂŞdimensional temperature
ϕ	Non âĂŞdimensional concentration
τ	Skin-friction coefficient

Subscripts

ω	Wall condition
∞	Free stream condition

past a semi-infinite vertical porous moving plate with variable suction. Chamkha [6] extended the work of Kim in which he discussed unsteady MHD convective heat and mass transfer past a semi-infinite vertical permeable moving plate with heat absorption. Alam et al. [7] discussed numerical study of the combined free forced convection and mass transfer flow past a vertical porous plate in a porous medium with heat generation and thermal diffusion.Sahin et al. [8] studied combined heat and mass transfer by mixed convection MHD flow along a porous plate with chemical reaction in presence of heat source.

Gebhar [9] has shown that the viscous dissipation effect plays an important role in natural convection in various devices that are subjected to large deceleration or that operate at high rotational speeds, in strong gravitational field processes on large scales (on large planets), and in geological processes. Soundalgekar [10] analyzed the effect

of viscous dissipative heat on the two dimensional unsteady, free convective flow past an vertical porous plate when the temperature oscillates in time and there is constant suction at the plate. Israel Cookey et al [11] investigated the influence of viscous dissipation and radiation on unsteady MHD free convection flow past an infinite heated vertical plate in porous medium with time dependent suction. Aurangzaib et al. [12] investigated the effect of thermal stratification on magnetohydrodynamic free convection boundary layer flow with heat and mass transfer of an electrically conducting fluid over an unsteady stretching sheet in the presence of strong magnetic field. The electron-atom collision frequency is assumed to be relatively high, so that the hall effect is assumed to be exist, while induced magnetic field is neglected. The transformed nonlinear boundary layer equations are solved numerically by applying Keller-box method. Bestman [13] examined the natural convection boundary layer with suction and mass transfer in a porous medium. His results confirmed the hypothesis that suction stabilizes the boundary layer and affords the most efficient method in boundary layer. Sivaiah and Srinivasa Raju [14] studied effect of heat and mass transfer flow with Hall current, heat source and viscous dissipation.

The object of the present paper is to study the transient magnetohydrodynamic free convection flow past a vertical porous plate in presence of viscous dissipation. The problem is governed by the system of coupled non-linear partial differential equations whose exact solutions are difficult to obtain, if possible. So, finite element method has been adopted for its solution, which is more economical from computational point of view.

2. Mathematical analysis

Consider the an unsteady free convective boundary layer flow of a viscous, incompressible, electrically conducting fluid past an infinite vertical porous plate in the presence of viscous dissipation is considered. The x'- axis is taken in the upward direction along the plate and y' axis normal to it. The physical model and coordinate system are shown in Fig. 1. A uniform magnetic field is applied in the direction perpendicular to the plate. Due to infinite length in

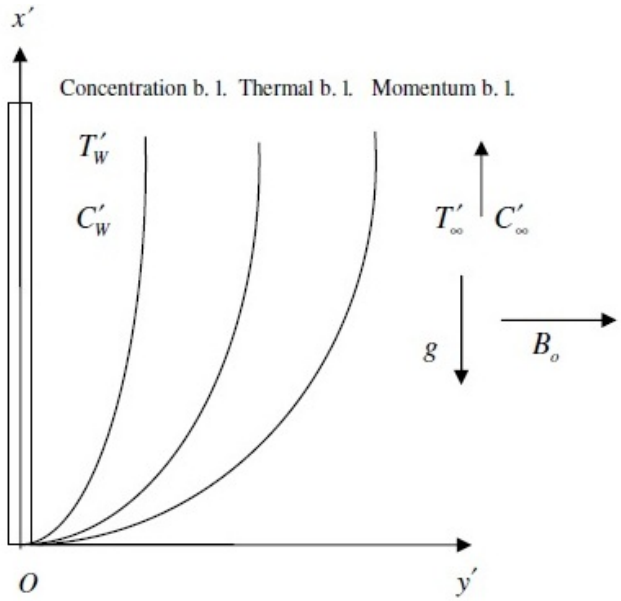

Fig. 1. Physical model and coordinate system

x'-direction, the flow variables are functions of y' and t' only. Under the usual Boussinesq approximation, governing equations for this unsteady problem are given by

$$\frac{\partial v'}{\partial y'} = 0 \tag{1}$$

$$\frac{\partial u'}{\partial t'} + v'\frac{\partial u'}{\partial y'} = -\frac{1}{\rho}\frac{\partial p'}{\partial x'} + \nu\frac{\partial^2 u'}{\partial y'^2} + g\beta(T' - T'_\infty) + g\beta^*(C' - C'_\infty) - \frac{\sigma B_0^2}{\rho}u' - \frac{\nu}{K'}u' \tag{2}$$

$$\frac{\partial T'}{\partial t'} + v'\frac{\partial T'}{\partial y'} = \frac{1}{\rho C_p}k\frac{\partial^2 T'}{\partial y'^2} + \frac{\nu}{C_p}(\frac{\partial u'}{\partial y'})^2 - \frac{S_0}{\rho C_p}(T' - T'_\infty) \tag{3}$$

$$\frac{\partial C'}{\partial t'} + v'\frac{\partial C'}{\partial y'} = D\frac{\partial^2 C'}{\partial y'^2} \tag{4}$$

Under these assumptions, the appropriate boundary conditions for the velocity, temperature and concentration fields are

$$t' < 0: \quad u' = 0, \quad T' = 0, \quad C' = 0 \quad \forall\, y',$$
$$t' \geq 0: \begin{cases} u' = u'_p, \quad T' = T'_\infty + \epsilon(T'_w - T'_\infty)e^{n't'} \quad C' = C'_\infty + \epsilon(C'_w - C'_\infty)e^{n't'} \text{ at } y' = 0, \\ u' = U'_\infty = U_0(1 + \epsilon A e^{n't'}), \quad T' \to T'_\infty, \quad C' \to C'_\infty \text{ as } y' \to \infty \end{cases} \tag{5}$$

From Eq. (1) it is clear that the suction velocity at the plate is either a constant or function of time only. Hence the suction velocity normal to the plate is assumed in the form

$$v' = -V_0(1 + \epsilon A e^{n't'}) \tag{6}$$

Where A is a real positive constant, ϵ and ϵA are small less than unity. Here V_0 is mean suction velocity, which has a non-zero positive constant and the minus sign indicates that the suction is towards the plate. Outside the boundary layer, Eq. (2) gives

$$\frac{-1}{\rho}\frac{\partial p'}{\partial x'} = \frac{dU'_\infty}{dt'} + \frac{\nu}{K'}U'_\infty + \frac{\sigma}{\rho}B_0^2 U'_\infty \tag{7}$$

In order to write the governing equations and the boundary conditions in dimensionless form, the following non-dimensional quantities are introduced.

$$u = \frac{u'}{U_0}, v = \frac{v'}{V_0}, \eta = \frac{V_0 y'}{\nu}, \; t = \frac{t' V_0^2}{\nu}, \; Pr = \frac{\rho C_p \nu}{k}, \; Sc = \frac{\nu}{D}, \theta = \frac{T' - T'_\infty}{T'_w - T'_\infty}, \; S = \frac{\nu S_0}{\rho C_p V_0^2}, \; n = \frac{\nu n'}{V_0^2},$$
$$\phi = \frac{C' - C'_\infty}{C'_w - C'_\infty}, \; K = \frac{K' V_0^2}{\nu^2}, \; Gr = \frac{g\beta\nu(T'_w - T'_\infty)}{U_0 V_0^2}, \; Gc = \frac{g\beta^*\nu(C'_w - C'_\infty)}{U_0 V_0^2}, \; M = \frac{\sigma B_0^2 \nu}{\rho V_0^2}, \; K = \frac{K'\nu}{V_0^2}, \tag{8}$$
$$E_c = \frac{U_0^2}{C_p(T'_w - T'_\infty)}, \; U_\infty = \frac{U'_\infty}{U_0}, \; U_p = \frac{u'_p}{U_0}$$

In view of Eqs. (5)-(8), Eqs. (2)-(4) reduce to the following dimensionless form:

$$\frac{\partial u}{\partial t} - (1 + \epsilon A e^{nt})\frac{\partial u}{\partial \eta} = \frac{dU_\infty}{dt} + Gr\theta + Gc\phi + \frac{\partial^2 u}{\partial \eta^2} + N(U_\infty - u) \tag{9}$$

$$\frac{\partial \theta}{\partial t} - (1 + \epsilon A e^{nt})\frac{\partial \theta}{\partial \eta} = \frac{1}{Pr}\frac{\partial^2 \theta}{\partial \eta^2} + E_c\left(\frac{\partial u}{\partial \eta}\right)^2 - S\theta \tag{10}$$

$$\frac{\partial \phi}{\partial t} - (1 + \epsilon A e^{nt})\frac{\partial \phi}{\partial \eta} = \frac{1}{Sc}\frac{\partial^2 \phi}{\partial \eta^2} \tag{11}$$

Where $N = M + \frac{1}{K}$.

The corresponding dimensionless boundary conditions are:

$$\begin{aligned} u = U_p, \theta = 1 + \epsilon\, e^{nt}, \phi = 1 + \epsilon\, e^{nt} \quad at \quad \eta = 0 \\ u \to U_\infty, \theta \to 0, \phi \to 0 \;\; as \;\; \eta \to \infty \end{aligned} \tag{12}$$

Now it is important to calculate the physical quantities of primary interest, which are the local shear stress, local surface heat flux and Sherwood number.

Dimensionless local wall shear stress or skin-friction is obtained as,

$$\tau = [\frac{\partial u}{\partial \eta}]_{\eta=0} \tag{13}$$

Dimensionless local surface heat flux or Nusselt number is obtained as,

$$Nu = [\frac{\partial \theta}{\partial \eta}]_{\eta=0} \tag{14}$$

Dimensionless the local Sherwood number is obtained as

$$Sh = [\frac{\partial \phi}{\partial \eta}]_{\eta=0} \tag{15}$$

3. Method of solution

The finite element method has been implemented to obtain numerical solutions of Eqs. (9)-(11) under boundary conditions (12). This technique is extremely efficient and allows robust solutions of complex coupled, nonlinear multiple degree differential equation systems. The fundamental steps comprising the method are now summarized. An excellent description of finite element formulations is available in Bathe [15] and Reddy [16]

Step-1: Discretization of the Domain into Elements

The whole domain is divided into finite number of "sub-domains", a process known as Discretization of the domain. Each sub-domain is termed a âĂIJfinite elementâĂİ. The collection of elements is designated the "finite element mesh".

Step-2: Derivation of the element Equations The derivation of finite element equations algebraic equations among the unknown parameters of the finite element approximation, involves the following three steps.

a. Construct the variational formulation of the differential equation.

b. Assume the form of the approximate solution over a typical finite element.

c. Derive the finite element equations by substituting the approximate solution into variational formulation.

These steps results in a matrix equation of the form $[K^e]\{u^e\}=\{F^e\}$, which defines the finite element model of the original equation.

Step-3 Assembly of Element Equations

The algebraic equations so obtained are assembled by imposing the âĂIJinter-elementâĂİ continuity conditions. This yields a large number of algebraic equations constituting the âĂIJglobal finite element modelâĂİ, which governs the whole flow domain.

Step-4:Impositions of Boundary Conditions

The physical boundary conditions defined in (12) are imposed on the assembled equations

Step-5: Solution of the Assembled Equations

The final matrix equation can be solved by a direct or indirect (iterative) method. For computational purposes, the coordinate is varied from to , where represents infinity external to the momentum, energy and concentration boundary layers. The whole domain is divided into a set of line segments of equal width each element being two-noded.

Variational formulation

The variational formulation associated with equations (9)-(11) over a typical two-noded linear element(η_e,η_{e+1}) is given by

$$\int_{\eta_e}^{\eta_{e+1}} w_1[(\frac{\partial u}{\partial t})-B(\frac{\partial u}{\partial \eta})-(\frac{\partial^2 u}{\partial \eta^2})-\frac{dU_\infty}{dt}+Nu-NU_\infty-Gr\theta-Gc\phi]d\eta=0 \tag{16}$$

$$\int_{\eta_e}^{\eta_{e+1}} w_2[(\frac{\partial \theta}{\partial t})-B(\frac{\partial \theta}{\partial \eta})-\frac{1}{Pr}(\frac{\partial^2 \theta}{\partial \eta^2})-S\theta-E_c(\frac{\partial u}{\partial t})^2]d\eta=0 \tag{17}$$

$$\int_{\eta_e}^{\eta_{e+1}} w_3[(\frac{\partial \phi}{\partial t})-B(\frac{\partial \phi}{\partial \eta})-\frac{1}{Sc}(\frac{\partial^2 \phi}{\partial \eta^2})]d\eta=0 \tag{18}$$

Where $B=1+\epsilon Ae^{nt}$ and w_1, w_2, w_3 are arbitrary test functions and may be viewed as the variation in u,θ and ϕ respectively. After reducing the order of integration and non-linearity, we arrive at the following system of equations

$$\begin{aligned}\int_{\eta_e}^{\eta_{e+1}} [(w_1)(\frac{\partial u}{\partial t})-B(w_1)(\frac{\partial u}{\partial \eta})+(\frac{\partial w_1}{\partial \eta})(\frac{\partial u}{\partial \eta})-(\frac{dU_\infty}{dt})(w_1)+N(w_1)u-N(w_1)U_\infty-\\ (Gr)(w_1)\theta-(Gc)(w_1)\phi]dy-[(w_1)(\frac{\partial u}{\partial \eta})]_{\eta_e}^{\eta_{e+1}}=0\end{aligned} \tag{19}$$

$$\int_{\eta_e}^{\eta_{e+1}} [(w_2)(\frac{\partial \theta}{\partial t})-B(w_2)(\frac{\partial \theta}{\partial \eta})+\frac{1}{Pr}(\frac{\partial w_2}{\partial \eta})(\frac{\partial \theta}{\partial \eta})-S(w_2)\theta-E_c(w_2)(\frac{\partial u}{\partial y})(\frac{\partial u}{\partial y})]d\eta-[(\frac{w_2}{Pr})(\frac{\partial \theta}{\partial \eta})]_{\eta_e}^{\eta_{e+1}}=0 \tag{20}$$

$$\int_{\eta_e}^{\eta_{e+1}} [(w_3)(\frac{\partial \theta}{\partial t})-B(w_3)(\frac{\partial \phi}{\partial \eta})-\frac{1}{Sc}(\frac{\partial w_3}{\partial \eta})(\frac{\partial \phi}{\partial \eta})]d\eta-[(\frac{w_3}{Sc})(\frac{\partial \phi}{\partial \eta})]_{\eta_e}^{\eta_{e+1}}=0 \tag{21}$$

Finite Element formulation

The finite element model may be obtained from Eqs. (20)-(21) by substituting finite element approximations of the form:

$$u=\sum_{j=1}^{2}u_j^e\psi_j^e,\quad \theta=\sum_{j=1}^{2}\theta_j^e\psi_j^e,\quad \phi=\sum_{j=1}^{2}\phi_j^e\psi_j^e \tag{22}$$

With $w_1=w_2=w_3=\psi_j^e(j=1,2)$, where u_j^e,θ_j^e and θ_j^e are the velocity, temperature and concentration respectively at the jth node of typical eth element (η_e,η_{e+1}) and ψ_i^e are the shape functions for this element (η_e,η_{e+1}) and are taken as:

$$\psi_1^e=\frac{\eta_{e+1}-\eta}{\eta_{e+1}-\eta_e}\ \ and\ \ \psi_2^e=\frac{\eta-\eta_e}{\eta_{e+1}-\eta_e},\ \ \eta_e\le\eta\le\eta_{e+1} \tag{23}$$

$$\begin{bmatrix}[K^{11}] & [K^{12}] & [K^{13}]\\ [K^{21}] & [K^{22}] & [K^{23}]\\ [K^{31}] & [K^{32}] & [K^{33}]\end{bmatrix}\begin{bmatrix}\{u^e\}\\ \{\theta^e\}\\ \{\phi^e\}\end{bmatrix}+\begin{bmatrix}[M^{11}] & [M^{12}] & [M^{13}]\\ [M^{21}] & [M^{22}] & [M^{23}]\\ [M^{31}] & [M^{32}] & [M^{33}]\end{bmatrix}\begin{bmatrix}\{u'^e\}\\ \{\theta'^e\}\\ \{\phi'^e\}\end{bmatrix}=\begin{bmatrix}\{b^{1e}\}\\ \{b^{2e}\}\\ \{b^{3e}\}\end{bmatrix} \tag{24}$$

where $\{[K^{mn}],[M^{mn}]\}$ and$\{\{u^e\},\{\theta^e\},\{\varphi^e\},\{u'^e\},\{\theta'^e\},\{\varphi'^e\}\ and\ \{b^{me}\}\}$ $(m,\ n=1,\ 2,\ 3)$ are the set of matrices of order 2×2 and 2×1 respectively and $'$ (dash) indicates $\frac{d}{d\eta}$. These matrices are defined as follows:

$$K_{ij}^{11}=-B\int_{\eta_e}^{\eta_{e+1}}[(\psi_i^e)(\frac{\partial\psi_j^e}{\partial\eta})]d\eta+\int_{\eta_e}^{\eta_{e+1}}[(\frac{\partial\psi_i^e}{\partial\eta})(\frac{\partial\psi_j^e}{\partial\eta})d\eta]+N\int_{\eta_e}^{\eta_{e+1}}[(\psi_i^e)(\psi_j^e)]d\eta,$$

$$K_{ij}^{12}=-[\frac{dU_\infty}{dt}+NU_\infty]\int_{\eta_e}^{\eta_{e+1}}[(\psi_i^e)d\eta,\ K_{ij}^{13}=-[Gr+Gc]\int_{\eta_e}^{\eta_{e+1}}[(\psi_i^e)(\psi_j^e)d\eta,\ M_{ij}^{11}=\int_{\eta_e}^{\eta_{e+1}}[(\psi_i^e)(\psi_j^e)d\eta,$$

$$M_{ij}^{12}=M_{ij}^{13}=0,\ K_{ij}^{21}=-E_c\int_{y_e}^{y_{e+1}}(\psi_i^e)(\frac{\partial u}{\partial y})(\frac{\partial\psi_j e}{\partial y})]dy,\ M_{ij}^{21}=M_{ij}^{23}=0,M_{ij}^{22}=\int_{\eta_e}^{\eta_{e+1}}(\psi_i^e)(\psi_j^e)d\eta,$$

$$K_{ij}^{31}=0,\ K_{ij}^{23}=S\int_{\eta_e}^{\eta_{e+1}}[(\psi_i^e)(\psi_j^e)]d\eta,\ M_{ij}^{31}=M_{ij}^{32}=0,\ M_{ij}^{33}=\int_{\eta_e}^{\eta_{e+1}}(\psi_i^e)(\psi_j^e)d\eta,$$

$$K_{ij}^{22}=-B\int_{\eta_e}^{\eta_{e+1}}[(\psi_i^e)(\frac{\partial\psi_j^e}{\partial\eta})]d\eta+\frac{1}{Pr}\int_{\eta_e}^{\eta_{e+1}}[(\frac{\partial\psi_i^e}{\partial\eta})(\frac{\partial\psi_j^e}{\partial\eta})d\eta],$$

$$K_{ij}^{32}=0,\ K_{ij}^{33}=-B\int_{\eta_e}^{\eta_{e+1}}[(\psi_i^e)(\frac{\partial\psi_j^e}{\partial\eta})]d\eta,b_i^{1e}=[(\psi_i^e)(\frac{\partial u}{\partial\eta})]_{\eta_e}^{\eta_{e+1}},$$

$$b_i^{2e}=[\frac{\psi_i^e}{Pr}(\frac{\partial\theta}{\partial\eta})]_{\eta_e}^{\eta_{e+1}},\ b_i^{3e}=[\frac{\psi_i^e}{Sc}(\frac{\partial\phi}{\partial\eta})]_{\eta_e}^{\eta_{e+1}}$$

The whole domain is divided into a set of 60 intervals of equal length 0.1. At each node 3 functions are to be evaluated. Hence after assembly of the elements we obtain a set of 143 equations. The system of equations after assembly of elements, are non-linear and consequently an iterative scheme is employed to solve the matrix system, which are solved using the Gauss Elimination method maintaining an accuracy of 0.0005.

4. Results and discussions

The formulation of the problem that accounts for the transient magnetohydrodynamic free convection flow past a vertical porous plate in presence of viscous dissipation is performed in the preceding sections. The governing equations of the flow field are solved numerically by using a finite element method. The above presented equations enable us to carry out numerical computations. The following parameter values are adopted for computations unless otherwise indicated in the figures and table: $Gr=2.0, Gc=1.0, M=0.0, K=0.5, Pr=0.7, S=1.0, E_c=0.001, Sc=0.6, U_p=0.5, A=0.5, \epsilon=0.2, n=0.1, t=1.0$. The boundary conditions for $\eta\longrightarrow\infty$ are replaced by those at η_{max} where the value of η_{max} is sufficiently large, so that the velocity at $\eta=\eta_{max}$ is equal to the relevant free stream velocity. We choose $\eta_{max}=6$. To assess the accuracy of the present method, comparisons between the present results and previously published data Chamkha [6], Table 1 shows the comparison between values of skin-friction coefficient τ. Table 2 shows the comparison between values of Nusselt number of Nu, also Table 3 shows the comparison between values of Sherwood number Sh . In fact, this results show a close agreement, hence an encouragement for further study of the effects of other varies of parameters on the continuous moving surface.

Figs. 2 and 3 exhibit the effect of thermal Grashof number and solutal Grashof numbers on the velocity profile with other parameters are fixed. The Grashof number signifies the relative effect of the thermal buoyancy force to the viscous hydrodynamic force in the boundary layer. As expected, it is observed that there is a rise in the velocity due to the enhancement of thermal buoyancy force. Also, as increases, the peak values of the velocity increases rapidly near the porous plate and then decays smoothly to the free stream velocity. The solutal Grashof number defines the ratio of the species buoyancy force to the viscous hydrodynamic force. As expected, the fluid velocity increases and the peak value is more distinctive due to increase in the species buoyancy force. The velocity distribution attains a distinctive maximum value in the vicinity of the plate and then decreases properly to approach the free stream value. It is noticed that the velocity increases with increasing values of the solutal Grashof number. The effect of the Hartmann number M is shown in Fig. 4. It is observed that the velocity of the fluid decreases with the increase of the magnetic field number values. The decrease in the velocity as the Hartmann number M increases is because the presence of a magnetic field in an electrically conducting fluid introduces a force called the Lorentz force, which acts against the flow if the magnetic field is applied in the normal direction, as in the present study. This resistive force slows down the fluid velocity component as shown in Fig. 4. The Permeability parameter K as defined in Eq. (5) is inversely proportional to the actual permeability KâĂš of the porous medium. An increase in K will therefore increase the resistance of the porous medium (as the permeability physically becomes less with increasing KâĂš) which will tend to accelerate the flow and increases the velocity. This behavior is evident from Fig. 5.

The effect of the viscous dissipation parameter i.e., the Eckert number E_c on the velocity and temperature are shown in Figs. 6 and 7 respectively. Eckert number is the ratio of the kinetic energy of the ïňĆow to the boundary layer enthalpy deference. It embodies the conversion of kinetic energy into internal energy by work done against the viscous fluid stresses. The positive Eckert number implies cooling of the plate i.e., loss of heat from the plate to the fluid. Hence, greater viscous dissipative heat causes a rise in the temperature as well as the velocity, which is evident from Figs. 6 and 7.

Figs. 8 and 9 illustrate the influence of heat absorption parameter on the velocity and temperature at t = 1.0 respectively. Physically speaking, the presence of heat absorption (thermal sink) effects has the tendency to reduce the fluid temperature. This causes the thermal buoyancy effects to decrease resulting in a net reduction in the fluid velocity. These behaviors are clearly obvious from Figs. 8 and 9 in which both the velocity and temperature distributions decrease as S increases. It is also observed that the both the hydrodynamic (velocity) and the thermal (temperature) boundary layers decrease as the heat absorption effects increase. The effect of Schmidt number Sc on the velocity and concentration are shown in Figs. 10 and **??**. As the Schmidt number increases, the velocity and concentration decreases. This causes the concentration buoyancy effects to decrease yielding a reduction in the fluid velocity. Reductions in the velocity and concentration distributions are accompanied by simultaneous reductions in the velocity and concentration boundary layers.

Table 1-Table 3 depict the effects of the solutal Grashof number Gc , the heat absorption coefficient S and the Schmidt number Sc on the skin-friction coefficient τ , Nusselt number Nu and the Sherwood number Sh , respectively. It is observed from these tables that as Gc increases, the skin-friction coefficient increases whereas the Nusselt and Sherwood numbers remain unchanged. However, as the heat absorption effects increase, both the skin-friction coefficient and the Nusselt number decrease whereas the Sherwood number remains unaffected. Also, increases in the Schmidt number cause reductions in the skin-friction coefficient and the Sherwood number while the Nusselt number remains constant.

Table 1. Effects of Gr on Skin-friction, Nusselt number and Sherwood number when $E_c = 0$.

Gr	Present results			Previous results of Ali J Chamka [6]		
	τ	Nu	Sh	τ	Nu	Sh
0.0	2.7200	-1.7167	-0.8098	2.7200	-1.7167	-0.8098
1.0	3.2772	- 1.7167	-0.8098	3.2772	-1 .7167	-0.8098
2.0	3.8343	-1.7167	-0.8098	3.8343	-1.7167	-0.8098
3.0	4.3915	-1.7167	-0.8098	4.3915	-1.7167	-0.8098
4.0	4.9487	-1.7167	-0.8098	4.9487	-1.7167	-0.8098

Table 2. Effects of S on Skin-friction,Nusselt number and Sherwood number when $E_c = 0$.

S	Present results			Previous results of Ali J Chamka [6]		
	τ	Nu	Sh	τ	Nu	Sh
0.0	3.4595	-1.7167	-0.8098	2.7200	-1.7167	-0.8098
1.0	3.2772	-1.7167	-0.8098	3.2772	-1.7167	-0.8098
2.0	3.1933	-2.1193	-0.8098	3.1933	-2.1193	-0.8098
3.0	3.1378	-2.4388	-0.8098	3.1378	-2.4388	-0.8098

Table 3. Effects of Sc on Skin-friction, Nusselt number and Sherwood number when $E_c = 0$.

Sc	Present results			Previous results of Ali J Chamka [6]		
	τ	Nu	Sh	τ	Nu	Sh
0.16	3.4328	-1.7167	-0.2231	3.4328	-1.7167	-0.2231
0.6	3.2772	-1.7167	-0.8098	3.2772	-1.7167	-0.8098
1.0	3.1847	-1.7167	-1.3425	3.1847	-1.7167	-1.3425
2.0	3.0481	-1.7167	-2.6741	3.0481	-1.7167	-2.6741

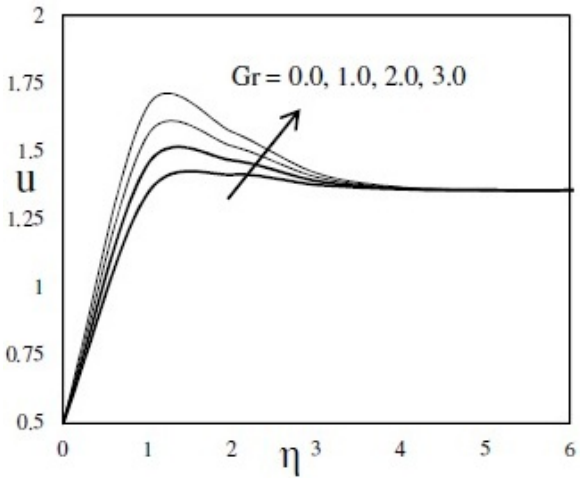

Fig. 2. Effect of Gr on velocity profiles

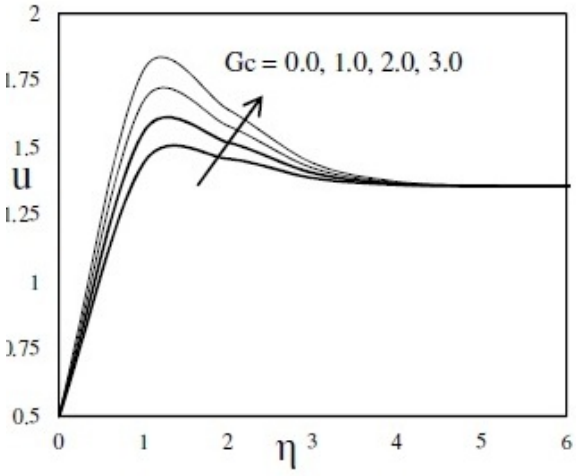

Fig. 3. Effect of Gc on velocity profiles

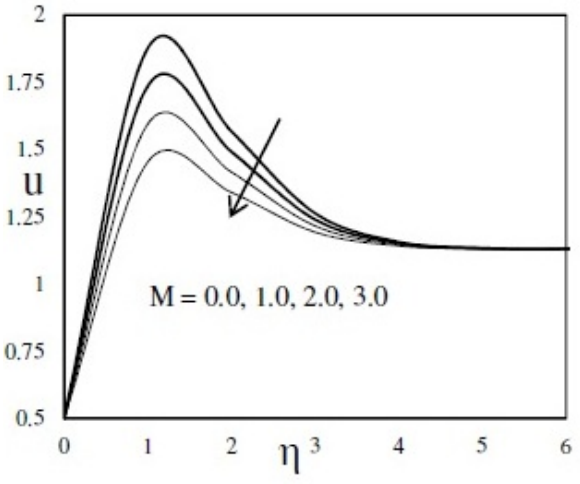

Fig. 4. Effect of M on velocity profiles

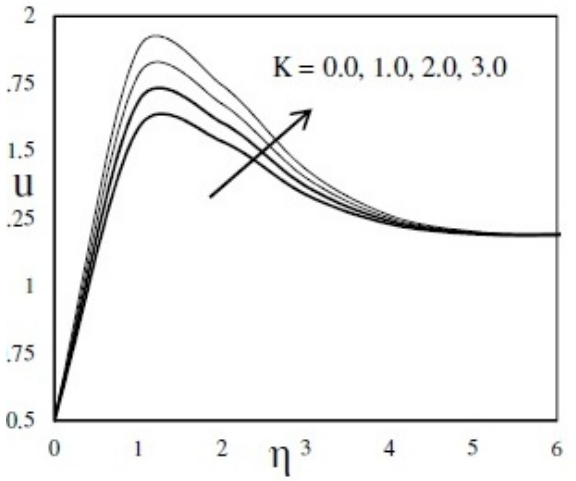

Fig. 5. Effect of K on velocity profiles

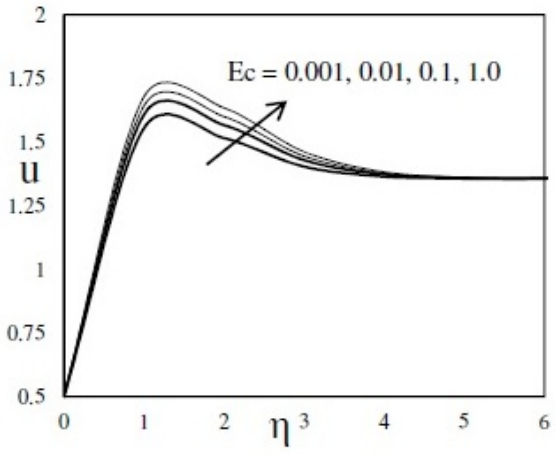

Fig. 6. Effect of E_c on velocity profiles

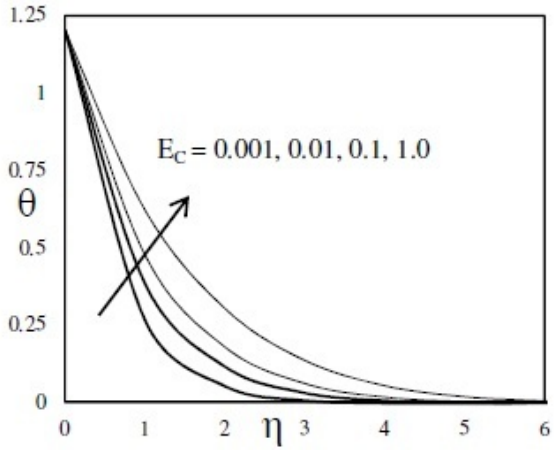

Fig. 7. Effect of E_c on temperature profiles

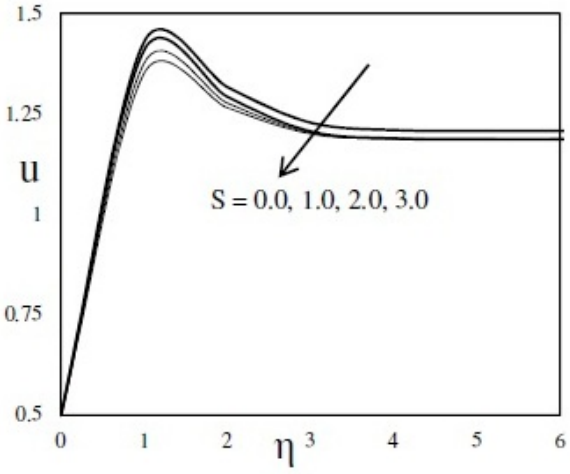

Fig. 8. Effect of S on velocity profiles

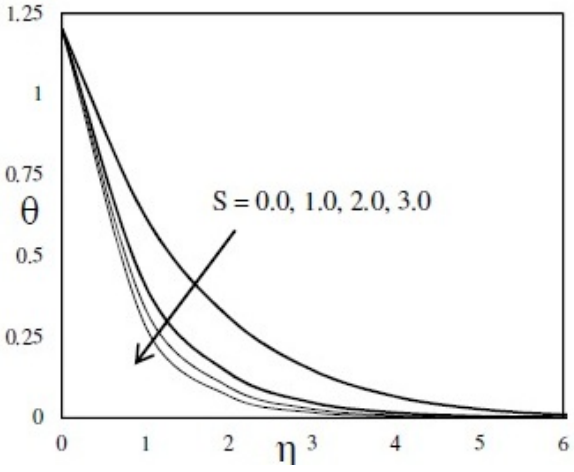

Fig. 9. Effect of S on temperature profiles

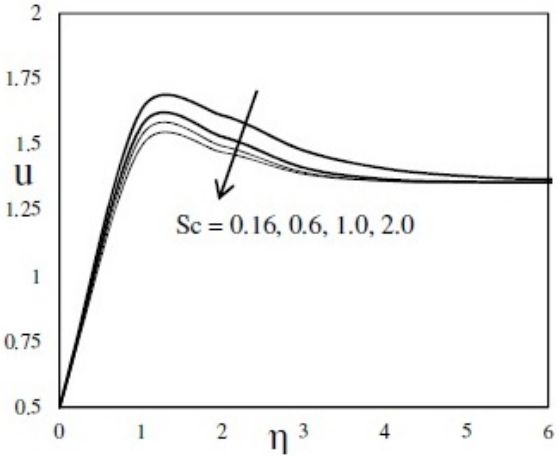

Fig. 10. Effect of Sc on velocity profiles

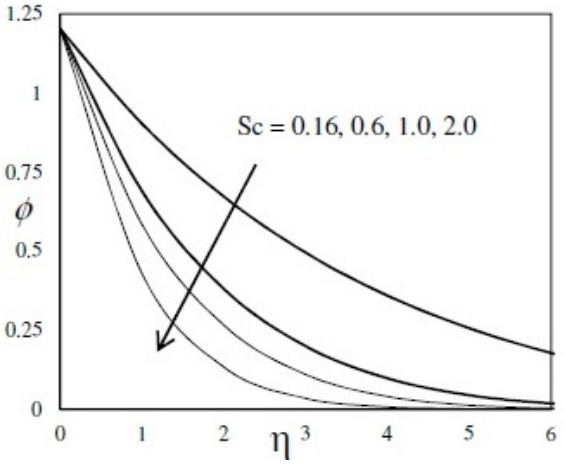

Fig. 11. Effect of Sc on concentration profiles

5. Conclusion

This paper considered transient magnetohydrodynamic free convection flow past a vertical porous plate in presence of viscous dissipation. The non-dimensional governing equations are solved with the help of finite element method, which have wide application in different fields of engineering. The conclusions of the study are as follows:

1. The velocity increases with the increase in thermal Grashof number and solutal Grashof number.
2. The velocity decreases with an increase in the magnetic parameter.
3. The velocity increases with an increase in the permeability of the porous medium parameter.
4. An increase in the Eckert number increases the velocity and temperature.
5. Increasing the heat absorption parameter reduces both velocity and temperature.
6. The velocity as well as concentration decreases with an increase in the Schmidt number

Acknowledgments

The authors are thankful to the University Grant Commission, New Delhi, India for providing financial assistance to carry out this research work under UGC - Major Research Project [F.No.42-22/2013(SR)].

References

[1] D. Ingham, I. Pop, (Eds.) Transport phenomena in porous media, Pergamon, Oxford. Vol.I. 1998 and Vol.II. 2002.
[2] D. A. Nield, A. Bejan, Convection in Porous Media, Second ed., Springer, New York, 1999.
[3] K. Vafai (Ed.), Handbook of Porous Media, Marcel Dekker, New York, 2000. 5
[4] I. Pop, D. Ingham, Convective heat transfer, mathematical and computational modeling of viscous fluids and porous media, Pergamon, Oxford, 2001.
[5] J. Youn.Kim, Unsteady MHD convective heat transfer past a semi-infinite vertical porous moving plate with variable suction, Int.J.Eng.Sci.38(2000) 833–845
[6] J. Ali.Chamkha, Unsteady MHD convective heat and mass transfer past a semi-infinite vertical permeable moving plate with heat absorption, Int.J.Eng.Sci.42(2004) 217–230.
[7] Numerical study of the combined free forced convection and mass transfer flow past a vertical porous plate in a porous medium with heat generation and thermal diffusion, Nonlinear Analysis: Modeling and control. 11(4)(2006) 331–343.
[8] Sahin Ahamed, J. Zueco, Combined heat and mass transfer by mixed convection MHD flow along a porous plate with Chemical reaction in presence of heat source, Applied Mathematics and Mechanics. 31(2010) 1217–1230.
[9] B. Gebhar, Effects of Viscous Dissipative in Natural Convection, Journal of Fluid Mechanics. 14(1962) 225-232.
[10] V.M. Soundalgekar, Viscous Dissipative Effects on Unsteady free Convective Flow Past an Vertical Porous Plate with Constant Suction, Int. J. Heat and Mass Transfer. 15(1972) 1253–1261.
[11] C. Israel-Cookey, A. Ogulu, V.B. Omubo-Pepple,Influence of Viscous Dissipation on Unsteady MHD free Convection Flow Past an Infinite Heated Vertical Plate in Porous Medium with Time Dependent Suction, Int. J. Heat and Mass Transfer. 46(2003) 2305–2311.
[12] A.R.M. Aurangzaib Kasim, N.F. Mohammad, Sheridan ShaïňĄe, Effect of thermal stratiïňĄcation on MHD free convection with heat and mass transfer over an unsteady stretching surface with heat source Hall current and chemical reaction, Int. J. Adv. Eng. Sci. Appl. Math. 4(2012) 217–225.
[13] A.R. Bestman, Natural convection boundary layer with suction and mass transfer in a porous medium, Int. J. Energy Res. 14(1990) 389–396.
[14] S. Sivaiah, R. Srinivasa Raju, Finite element solution of heat and mass transfer flow with Hall current heat source and viscous dissipation, Appl. Math and Mech. 34(2013) 559–570.
[15] K.J. Bathe, Finite Element Procedures, Prentice-Hall. New Jersey, 1996.
[16] J.N. Reddy, An Introduction to the Finite Element Method, McGraw-Hill Book Company, 3rd Edition, New York, 2006.